Effect of matrix cracking on the overall thermal conductivity of fibre-reinforced composites

By T. J. Lu and J. W. Hutchinson
Division of Applied Sciences, Harvard University, Cambridge, MA 02138, USA

The longitudinal thermal conductivity of a unidirectional fibre-reinforced composite containing an array of equally spaced transverse matrix cracks is calculated. The cracked composite is modelled by a cylindrical cell which accounts for altered heat transfer across the matrix cracks as well as through debonded portions of the fibre–matrix interface. Heat transfer mechanisms across the cracks and dedonded interfaces considered are contact, gaseous conduction, and radiation, and the relative importance of these mechanisms is discussed. Approximate closed form solutions to the cell model for the overall thermal conductivity are obtained using an approach reminiscent of the shear lag analysis of stiffness loss due to matrix cracking and debonding. Selected numerical results from a finite-element analysis of the cell model are presented to complement the analytical solutions. Both matrix cracking and interfacial debonding have the potential for significantly reducing the longitudinal thermal conductivity.

1. Introduction

The rule of mixtures holds rigorously for the overall longitudinal thermal conductivity k_z^0 of a crack-free composite reinforced by continuous unidirectional fibres: $k_z^0 = \rho k_z^{\mathrm{f}} + (1-\rho)k_{\mathrm{m}}$, where is ρ the fibre volume fraction, k_z^{f} is the axial thermal conductivity of the fibre and k_{m} is the matrix conductivity. This result continues to apply when fibre debonding occurs (i.e. when a thermal barrier of negligible thickness emerges at the debonded portion of the fibre–matrix interface) but fails if the matrix develops cracks perpendicular to the fibres which impede the heat flow. Such matrix cracking may occur in intermetallic and ceramic matrix composites, arising from excessive stressing in the vicinity of notches or other sources of stress concentrations. Thus, the presence of these matrix cracks will degrade the thermal conductivity of the composite and thereby alter heat flow. In the extreme, heat transfer through the matrix can be fully interrupted by a combination of matrix cracking and interfacial debonding such that the overall longitudinal thermal conductivity of the composite is due entirely to heat conducted by the intact fibres. It is evident, therefore, that the longitudinal conductivity will range from k_z^0 for the uncracked composite to as little as ρk_z^{f} when matrix cracking and interface debonding reduce the effective heat flow in the matrix to zero. Matrix cracking also strongly affects other thermo-mechanical properties of the compo-

Phil. Trans. R. Soc. Lond. A (1995) **351**, 595–610
Printed in Great Britain

TEX Paper

site such as stiffness, coefficients of thermal expansion (CTE), thermal diffusivity, etc. These issues are now receiving increased attention in connection with the application of composite materials to environments involving high temperatures and temperature gradients.

Several analytical procedures have been developed for the evaluation of the overall thermal conductivity of a homogeneous, isotropic matrix containing distributed, weakly interacting cracks or voids (e.g. Hasselman 1978; Hoenig 1983; Tzou 1991; Tzou & Li 1993). For a unidirectional fibre-reinforced matrix composite suffering no matrix cracking, the influence of fibre–matrix debonding on the overall transverse thermal conductivity of the material has been studied by Benveniste (1987), Hasselman & Johnson (1987), Bhatt *et al.* (1990) and Fadale & Taya (1991), among others. In the case where the fibres are perfectly bonded to the matrix with intimate thermal contact across their interface or in the case where full debonding along the fibre–matrix interface occurs, the presence of matrix cracking perpendicular to the fibres does not affect the thermal conductance capability of the composite in the transverse direction. Thus in the analysis to follow the focus is on the overall longitudinal thermal conductivity of the unidirectional composite as influenced by matrix cracking and interface debonding.

The key element in building up a solution to the titled problem is the determination of the disturbance to the temperature distribution in each composite constituent due to the matrix cracks and the debonded interfaces. The thermal conductance mechanisms that are in play across the cracks and the debonded interfaces will be discussed. The same cylindrical cell is used to model the conductivity of the cracked composite as was used by He *et al.* (1994) to predict tensile stress–strain behaviour and by Lu & Hutchinson (1995) to study CTE changes. The present study will focus on a composite comprised of transversely isotropic fibres in an isotropic matrix such that the effective properties of the composite are transversely isotropic relative to the fibre direction. Attention is mainly directed to systems where the matrix has a larger thermal expansion coefficient than those of the fibres, such that upon cooling from the processing temperature, residual tension builds up in the matrix parallel to the fibres while compression develops across the fibre–matrix interfaces. As a consequence, once formed, the matrix cracks remain open, and debonded portions of the fibre–matrix interfaces remain nominally closed but with reduced thermal contact. The thermal barrier at the debonded interfaces is modelled by an equivalent interfacial heat transfer coefficient comprised of the sum of three conductances: fibre–matrix contact across the interface, gaseous conduction and radiation heat exchange. Only the latter two mechanisms operate to transfer heat across the matrix cracks. Based on the analogy between the variables describing elasticity and those for steady-state heat conduction, an approximate analytical solution for the effective thermal conductivity as a function of crack density is obtained by an approach analogous to the well-known shear lag analysis of stiffness loss due to matrix cracking and interface debonding. The accuracy of the approximations introduced in the analysis of the cell model will be assessed with the aid of selected finite-element calculations.

The organization of the paper is as follows. In § 2, the problems are formulated with discussion of the heat transfer boundary conditions. Solutions for the overall thermal conductivity of the cracked composite with perfect fibre–matrix bonding are derived in § 3. These results are extended in § 4 to account for the combined effects of matrix cracking and interface debonding.

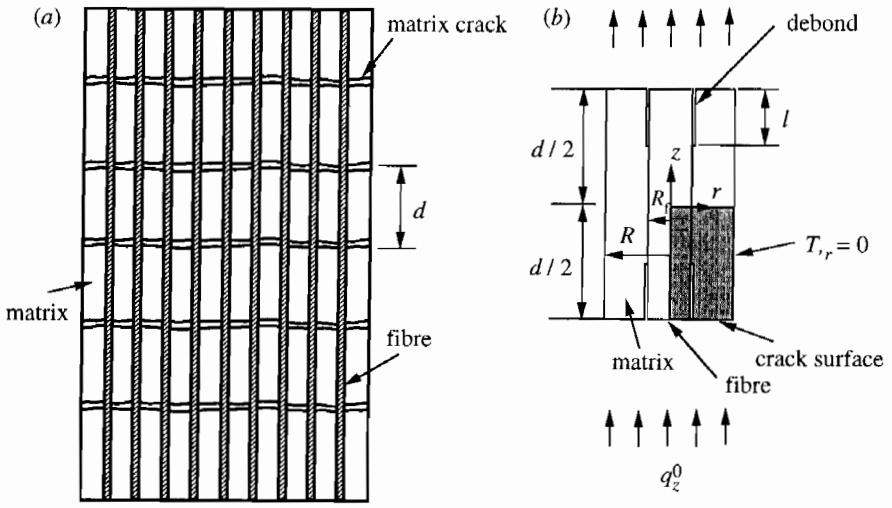

Figure 1. (*a*) A unidirectionally reinforced fibre–matrix composite with an array of uniformly spaced matrix cracks; and (*b*) a single unit cell of the periodically cracked composite.

2. Formulation of the problems

A unidirectional, continuous fibre-reinforced composite has through-the-thickness, periodically distributed matrix cracks with spacing d, as depicted in figure 1*a*. For cases in which fibre–matrix debonding has occurred, the debonds extending from the matrix crack surfaces will be assumed to have a common length l such that the periodicity is preserved. The average heat flux in the composite parallel to the fibres is denoted by q_z^0. The cylindrical cell shown in figure 1*b* is introduced to model one of the periodic cells of the cracked composite. Boundary conditions appropriate to the cylindrical cell will be discussed below. A set of cylindrical polar coordinates (r, θ, z) is chosen such that the z-axis coincides with the axis of the fibre and increases in the direction of the heat flow, with $z = 0$ at the cell centre. The radius R of the cylindrical cell is related to the fibre radius R_f via $R = R_\mathrm{f}/\sqrt{\rho}$. Debonding over a cylindrical portion of the fibre–matrix interface, if present, is modelled by an interfacial crack extending a distance l on either side of each matrix crack surface. It follows that $l = \frac{1}{2}d$ represents complete debonding, whereas $l = 0$ corresponds to no debonding.

(*a*) *Basic heat conduction equations*

By cylindrical symmetry, the temperature and temperature gradient fields in the cell depend only on r and z. For fibres with transversely isotropic properties, Fourier's law reads

$$\begin{Bmatrix} q_r^\mathrm{f} \\ q_z^\mathrm{f} \end{Bmatrix} = -\begin{bmatrix} \gamma k_z^\mathrm{f} & 0 \\ 0 & k_z^\mathrm{f} \end{bmatrix} \begin{Bmatrix} T_{\mathrm{f},r} \\ T_{\mathrm{f},z} \end{Bmatrix}, \tag{2.1}$$

where $q_r^\mathrm{f}(r, z)$ and $q_z^\mathrm{f}(r, z)$ are flux components in the radial and axial directions, k_r^f $(= \gamma k_z^\mathrm{f})$, k_z^f are transverse and longitudinal thermal conductivities of the fibre, $T_\mathrm{f}(r, z)$ is the current temperature in the fibre, $T_{\mathrm{f},r} \equiv \partial T_\mathrm{f}/\partial r$, etc. The corresponding relation for the isotropic matrix is

$$\begin{Bmatrix} q_r^\mathrm{m} \\ q_z^\mathrm{m} \end{Bmatrix} = -\begin{bmatrix} k_\mathrm{m} & 0 \\ 0 & k_\mathrm{m} \end{bmatrix} \begin{Bmatrix} T_{\mathrm{m},r} \\ T_{\mathrm{m},z} \end{Bmatrix}, \tag{2.2}$$

with k_{m} designating the thermal conductivity of the matrix. In the analysis, $(k_{\mathrm{m}}, k_r^{\mathrm{f}}, k_z^{\mathrm{f}})$ are taken to be temperature-independent constants.

In the absence of internal heat sources, conservation of heat in association with Fourier's law (2.1) leads to the following steady-state equation of heat conduction in the fibre:

$$\frac{1}{r}\frac{\partial}{\partial r}\left(\gamma r\frac{\partial T_{\mathrm{f}}}{\partial r}\right)+\frac{\partial^2 T_{\mathrm{f}}}{\partial z^2}=0. \tag{2.3}$$

This equation also holds for the matrix material except for the replacement of fibre temperature $T_{\mathrm{f}}(r,z)$ by matrix temperature $T_{\mathrm{m}}(r,z)$ and $\gamma=1$. For isotropic fibres, equation (2.3) reduces to the more familiar Laplace equation.

The perfectly bonded portion of the interface is assumed to have no thermal resistance, requiring

$$\gamma k_z^{\mathrm{f}} T_{\mathrm{f},r}=k_{\mathrm{m}}T_{\mathrm{m},r} \qquad \text{on} \quad r=R_{\mathrm{f}}, \quad |z|\leqslant \tfrac{1}{2}d-l, \tag{2.4}$$

$$T_{\mathrm{f}}=T_{\mathrm{m}} \qquad \text{on} \quad r=R_{\mathrm{f}}, \quad |z|\leqslant \tfrac{1}{2}d-l, \tag{2.5}$$

Symmetry with respect to the z-axis implies:

$$T_{\mathrm{f},r}=0 \quad \text{on} \quad r=0, \quad |z|\leqslant \tfrac{1}{2}d. \tag{2.6}$$

The appropriate condition on the outer surface of the cell which models the periodic structure of the solution expected for the cracked composite of figure 1*a* is that no heat is transferred there, i.e.

$$T_{\mathrm{m},r}=0 \quad \text{on} \quad r=R, \quad |z|\leqslant \tfrac{1}{2}d. \tag{2.7}$$

Inside the cylindrical cell, on every cross-section transverse to the axis of the fibre, the following heat balance condition is satisfied:

$$(1-\rho)k_{\mathrm{m}}\hat{T}_{\mathrm{m},z}+\rho k_z^{\mathrm{f}}\hat{T}_{\mathrm{f},z}=-q_z^0 \quad \text{for} \quad |z|<\tfrac{1}{2}d, \tag{2.8}$$

where

$$\hat{T}_{\mathrm{f},z}=\frac{2}{R_{\mathrm{f}}^2}\int_0^{R_{\mathrm{f}}} rT_{\mathrm{f},z}\,\mathrm{d}r, \qquad \hat{T}_{\mathrm{m},z}=\frac{2}{R^2-R_{\mathrm{f}}^2}\int_{R_{\mathrm{f}}}^{R} rT_{\mathrm{m},z}\,\mathrm{d}r \tag{2.9}$$

are temperature gradients averaged over the cross-sectional areas of the fibre and matrix, respectively. Simple arguments based on the periodicity and linearity of the temperature field of the cracked (and possibly debonded) composite cell model disclose that the temperature distribution is independent of r on each of the transverse planes half way between the matrix cracks such as those at $z=0$ and $z=d$. It is also independent of r within the fibre on all planes containing matrix cracks such as $z=\frac{1}{2}d$. Denote by ΔT the temperature change between $z=0$ and $z=d$. The overall longitudinal thermal conductivity k_z is defined by

$$k_z=-\frac{q_z^0}{\Delta T/d}. \tag{2.10}$$

Apart from the conditions on the matrix crack surfaces and on the debonded portions of the fibre–matrix interface, which will be discussed immediately below, these equations fully specify the problem for k_z.

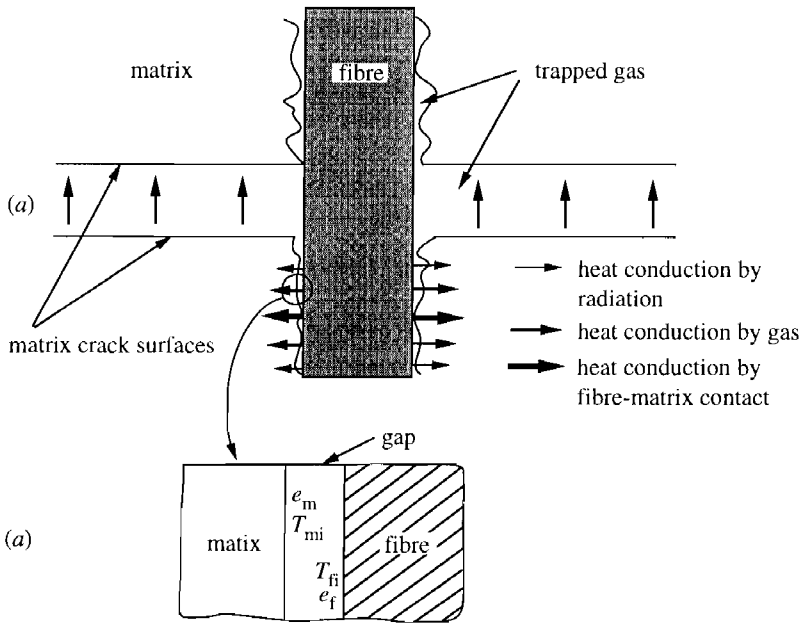

Figure 2. (*a*) Schematics of the heat conductance mechanisms across the matrix crack surfaces and the debonded portions of the fibre matrix interface; and (*b*) model representation of the radiative heat exchange between fibre and matrix over a typical gap at the interface.

(*b*) *Boundary condition at the debonded interfaces*

Heat flow will be impeded on portions of the fibre–matrix interface which have debonded. Assume the heat flow through the interface is proportional to the temperature jump across it. Let h_i be the *interfacial thermal conductance* defined such that

$$\gamma k_z^f T_{f,r} = k_m T_{m,r} = h_i(T_{mi} - T_{fi}) \quad \text{on} \quad r = R_f, \quad \tfrac{1}{2}d - l \leqslant |z| \leqslant \tfrac{1}{2}d, \qquad (2.11)$$

where $T_{fi}(z)$ and $T_{mi}(z)$ denote respectively the temperatures of the fibre and matrix at the interface. If the mechanisms of heat transfer through the interface operate independently, h_i can be written as (Leung & Tam 1988; Bhatt *et al.* 1990)

$$h_i = h_c + h_g + h_r, \qquad (2.12)$$

where h_c is the component contributed by heat transfer through contacting points between the fibre and matrix, h_g is due to the interfacial gaseous heat transfer, and h_r is attributable to the radiative heat transfer across the non-contacting portions of the interface (figure 2*a*). The subject of thermal resistance is itself a complex one, and no complete theory is available. Several theoretical models as well as experimental results for solid–solid interfaces are reviewed recently by Swartz & Pohl (1989).

Assuming the matrix has a larger thermal expansion coefficient than that of the fibre, the fraction of interfacial conductance due to fibre–matrix contact h_c depends in a complicated manner on both on the surface roughness of the debonded portion of the interface and on the clamping pressure σ_r acting over the interface. Since the latter scales with thermal expansion mismatch between fibre and matrix, it is expected that h_c should increase with mismatch. Quantitative estimates

of h_c are difficult to establish theoretically, but may often be inferred from the measurement of the total conductance h_i in vacuum, as will be discussed.

The detailed mechanism underlying the transfer of heat by the gas filling the spaces of the interface is controlled by the Knudsen number N_K, defined as the ratio of the mean free path of the gas to the characteristic width of the interfacial gap. When $N_K \ll 1$, the continuum theory of heat conduction in the gas applies. If $N_K \gg 1$ the energy exchange involves collisions of gas molecules and the interfacial surface with relatively few intervening interatomic or intermolecular collisions. For intermediate values of N_K, the two processes are in transition. Since the mean free path of a gas depends on both temperature and pressure, the mechanism controlling h_g may shift as environmental conditions imposed on the composite change.

To gain insight into the radiative heat transfer mode, consider radiative heat exchange between two parallel surfaces with emissivities e_m and e_f and absolute surface temperatures T_{mi} and T_{fi}, respectively, as depicted in figure 2*b*. The net rate of radiative heat exchange between the two surfaces is given by

$$q = \frac{\sigma(T_{fi}^4 - T_{mi}^4)}{1 - e_m e_f (e_m + e_f)}, \tag{2.13}$$

where $\sigma = 5.67 \times 10^{-8}$ W m^{-2} K^{-4} is the Stefan–Boltzmann constant of radiation. The temperature jump $T_{fi} - T_{mi}$ across the thin interfacial gap is expected to be small compared to either of the two surface temperatures. With $\bar{T}_i$ denoting the average of T_{mi} and T_{fi}, (2.13) can be approximated by

$$q_{ri} = \frac{4\sigma(\bar{T}_i)^3}{1 - e_m e_f (e_m + e_f)}(T_{fi} - T_{mi}), \tag{2.14}$$

which, in the light of (2.11) and (2.12), yields

$$h_r \propto \frac{4\sigma(\bar{T}_i)^3}{1 - e_m e_f (e_m + e_f)}. \tag{2.15}$$

As an estimation of the relative significance of the radiative effect, take $e_m = e_f = 0.9$ and $\bar{T}_i = 1200$ K in (2.15) to get $h_r \approx 7.1 \times 10^2$ W m^{-2} K^{-1}. This is a very small value compared to values such as 10^5 W m^{-2} K^{-1} or larger expected for most ceramic and intermetallic matrix composites maintaining nominally closed debonded interfaces or even gas-filled open interfaces. One point of calibration is the value of h_i measured experimentally by Bhatt *et al.* (1990) for debonded interfaces of a composite consisting of double-coated SCS-6 SiC fibres within a reaction-bonded silicon nitride matrix. The thermal expansion mismatch of this composite system is such that the debonded interface is fully opened. Nevertheless, h_i was found to be in the range 10^4 to 10^5 W m^{-2} K^{-1}, with h_g overwhelming h_r. Thus it can be reasonably expected that the radiative component h_r will generally be negligible for temperatures as large as 1200 K and probably higher, especially for composites for which the debonded interface surfaces maintain nominal contact.

The competition between heat transfer by surface asperity contact and gaseous conduction vanishes under vacuum conditions with the gaseous phase removed. (Bhatt *et al.* (1990) used vacuum testing to elucidate the role of gaseous conduction in their study.) Thus, to a good approximation, the interfacial thermal

conductance measured in vacuum represents the contact conductance h_c. Then to obtain the component h_g, one may measure the total interfacial conductance h_i in the gaseous phase of interest and subtract h_c from it.

(*c*) *Boundary condition on the crack surfaces*

As has been already emphasized, attention is focused on composite systems where the CTE of the matrix exceeds that of the fibre. For composites with either a ceramic or intermetallic matrix, the fibres are usually bonded to the matrix at relatively high temperatures. Under cooling from the fabricating temperature, the matrix develops residual tension in the direction of the fibre while a clamping pressure acts across the fibre–matrix interface. When matrix cracks form they remain completely open even under no applied load. Residual crack openings are generally in the range 0.01 1 μm, depending on many factors including residual stress, extent of fibre debonding and sliding, and fibre diameter.

Assuming negligible heat loss due to flow of gas through the cracks (which is justified for crack openings as large as 0.1 mm), it follows that heat transfer across the crack surfaces is realized by two mechanisms: gaseous conduction and crack surface radiation. Hence, with H_c denoting the total conductance across the matrix crack,

$$H_c = H_g + H_r, \tag{2.16}$$

where H_g and H_r are defined in the same way as h_g and h_r. The qualitative arguments advanced above for the relative importance of the two conductance contributions apply here as well. Specifically, it can be expected that H_r will often play a minor role. In general, the boundary condition governing heat transfer across the matrix crack surface is

$$k_m T_{m,z} = H_c(T_m^+ - T_m) \quad \text{on} \quad |z| = \tfrac{1}{2}d, \quad R_f \leqslant r \leqslant R, \tag{2.17}$$

where the flow of heat is taken to be in the positive z-direction, and T_m^+ and T_m^- are temperatures on the upper and lower surfaces of the crack, respectively. Under the limiting condition in which negligible heat passes across the crack, the boundary condition becomes

$$k_m T_{m,z} = 0 \quad \text{on} \quad |z| = \tfrac{1}{2}d, \quad R_f \leqslant r \leqslant R. \tag{2.18}$$

Under this limit when the cracks act as perfectly insulating barriers, and, for the cell model, all the heat then passes the plane at $z = \frac{1}{2}d$ through the fibre, i.e.

$$\frac{2}{R_f^2}\int_0^{R_f} rT_{f,z}\,\mathrm{d}r = -\frac{q_z^0}{\rho k_z^f} \quad \text{on} \quad |z| = \tfrac{1}{2}d. \tag{2.19}$$

3. Thermal conductivity of cracked composites with perfectly bonded interfaces

The set of governing equations of steady-state heat conduction in a unidirectional fibre-reinforced composite, (2.1) (2.3), is formally analogous to that of the elasticity problem for the same composite, if q_i, $T_{,i}$, k_{ij} are respectively replaced by ϵ_{ij}, σ_{ij}, S_{ijkl}. The so-called shear lag approximations (Laws & Dvorak 1988; McCartney 1990; Lu & Hutchinson 1995), which are very effective for estimating stiffness loss due to matrix cracking and debonding, can be adapted to the

thermal conductivity problem. Details of this approximate solution procedure are elaborated in an expanded version of this paper available from the second author as report MECH-239.

For perfectly bonded fibre–matrix interfaces, the governing differential equation which emerges for the average fibre temperature gradient in the presence of matrix cracking is

$$\frac{\mathrm{d}^2\hat{T}_{\mathrm{f},z}}{\mathrm{d}z^2} = \left(\frac{\xi}{R_{\mathrm{f}}}\right)^2 \left(\hat{T}_{\mathrm{f},z} + \frac{q_z^0}{k_z^0}\right) \quad \text{for} \quad |z| \leqslant \tfrac{1}{2}d, \tag{3.1}$$

where the non-dimensional coefficient is defined by

$$\xi = \{8\gamma k_z^0/(1-\rho)k_{\mathrm{m}}\}^{1/2}. \tag{3.2}$$

The relevant solution to (3.1) is

$$\hat{T}_{\mathrm{f},z} = -q_z^0/k_z^0 + A_1 \cosh(\xi z/R_{\mathrm{f}}) \quad \text{for} \quad |z| \leqslant \tfrac{1}{2}d, \tag{3.3}$$

where A_1 is a constant to be determined from the boundary condition. The first term is recognized as the uniform temperature gradient in the uncracked composite. The disturbance to the uniform field by the matrix cracks is represented by the second term. This same type of solution for this geometry carries over to problems of elasticity, thermal expansion, electrical conduction, electrostatics, and magnetostatics owing to the well known mathematical analogy that exists between the subjects (Batchelor 1974).

(*a*) *Thermally insulated crack surfaces*

If the matrix crack surfaces are thermally insulated under condition (2.18) discussed earlier, (3.3) together with (2.19) yields

$$\frac{\mathrm{d}\hat{T}_{\mathrm{f}}}{\mathrm{d}z} = -\frac{q_z^0}{k_z^0}\left\{1 + \frac{1-\rho}{\rho}\frac{k_{\mathrm{m}}}{k_z^{\mathrm{f}}}\frac{\cosh(\xi z/R_{\mathrm{f}})}{\cosh(\xi d/2R_{\mathrm{f}})}\right\} \quad \text{for} \quad |z| \leqslant \tfrac{1}{2}d. \tag{3.4}$$

The overall longitudinal thermal conductivity k_z is defined by (2.10) where $\Delta T = \hat{T}_{\mathrm{f}}(d) - \hat{T}_{\mathrm{f}}(0)$, since T is *uniform* with respect to r on $z = 0$ and $z = d$. Geometric symmetry with respect to $z = \frac{1}{2}d$ then gives

$$\Delta T = 2(\hat{T}_{\mathrm{f}}(\tfrac{1}{2}d) - \hat{T}_{\mathrm{f}}(0)) = 2\int_0^{d/2} \frac{\mathrm{d}\hat{T}_{\mathrm{f}}}{\mathrm{d}z}\,\mathrm{d}z. \tag{3.5}$$

(Equation (3.5) applies to the cell model for all boundary conditions considered in this paper.) By (2.10),

$$k_z = k_z^0\left\{1 + \frac{1-\rho}{\rho}\frac{k_{\mathrm{m}}}{k_z^{\mathrm{f}}}\frac{\tanh(\xi d/2R_{\mathrm{f}})}{\xi d/2R_{\mathrm{f}}}\right\}^{-1}. \tag{3.6}$$

Figure 3 gives curves of k_z/k_z^0 against normalized crack density R_{f}/d for five values of fibre volume fraction ρ: 0.1, 0.2, 0.3, 0.4 and 0.5. The constitutive parameters used in this example are $k_z^{\mathrm{f}}/k_{\mathrm{m}} = 2$ and $\gamma = 1$.

Also included in figure 3 are numerical results from a finite-element analysis of the boundary value problem for the cell as posed above for $\rho = 0.1$, 0.3, 0.5. The finite-element discretization is made for a quarter of the cell (the shaded region of figure 1*b*) with eight-node quadratic axisymmetric elements. Quarter-point elements are used to simulate the singular behaviour of the temperature

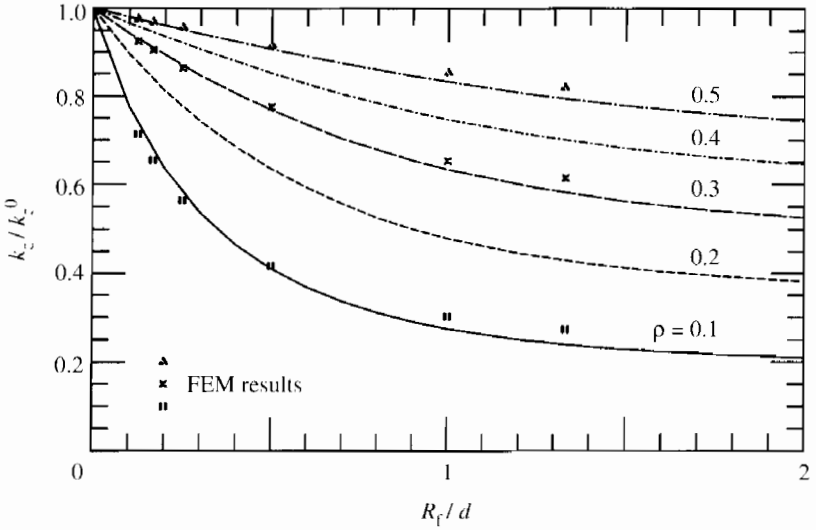

Figure 3. Cell model predictions and finite-element results for normalized longitudinal conductivity k_z/k_z^0 as functions of normalized crack density R_f/d for five selections of fibre volume fraction ρ: 0.1, 0.2, 0.3, 0.4 and 0.5. Other constitutive parameters used are $k_z^f/k_m = 2$, $\gamma = 1$ and $B_c = 0$.

gradient and heat flux fields in the vicinity of the crack tip. The agreement between the approximate solution and the finite-element results is clearly very good. For $d/R_f > 3$, the dependence of k_z on crack density is nearly linear. This is the density range in which interaction between neighbouring cracks is weak. At higher crack densities, k_z/k_z^0 decays relatively slowly and gradually approaches the asymptote $\rho k_z^f/k_z^0$. In the limit $d = 0$, all the heat flows through the fibre so that $k_z = \rho k_z^f$. The finite-element results are relatively insensitive to the details of the mesh around the crack tip when the crack density is low. They become more sensitive to mesh refinement at high densities, but, in any case, crack spacings less than about $2R_f$ are rare.

In passing, it is worth noting that (3.6) is similar in form to the shear lag approximation for the longitudinal elastic modulus E_z of the cracked unidirectional composite,

$$E_z = E_z^0 \left\{ 1 + D_1^0 \frac{R_f}{d} \tanh\left(\frac{S}{D_1^0} \frac{d}{R_f} \right) \right\}^{-1}, \tag{3.7}$$

where E_z^0 is the axial elastic modulus of the uncracked composite, and where D_1^0 and S are dimensionless functions of ρ and moduli ratios (Lu & Hutchinson 1995). Application of the shear lag approach to the stiffness problem requires some numerical analysis to evaluate D_1^0. Similar numerical work is unnecessary for the lower order heat conduction problem.

(*b*) *The effect of gaseous heat conduction within matrix cracks*

Gaseous conduction is expected to be the most important mechanism for heat transfer across the open matrix cracks, as previously discussed. Condition (2.17) is assumed to hold on the cracks where H_c is the heat conductance coefficient. This coefficient will be taken to be independent of the temperature in the analysis,

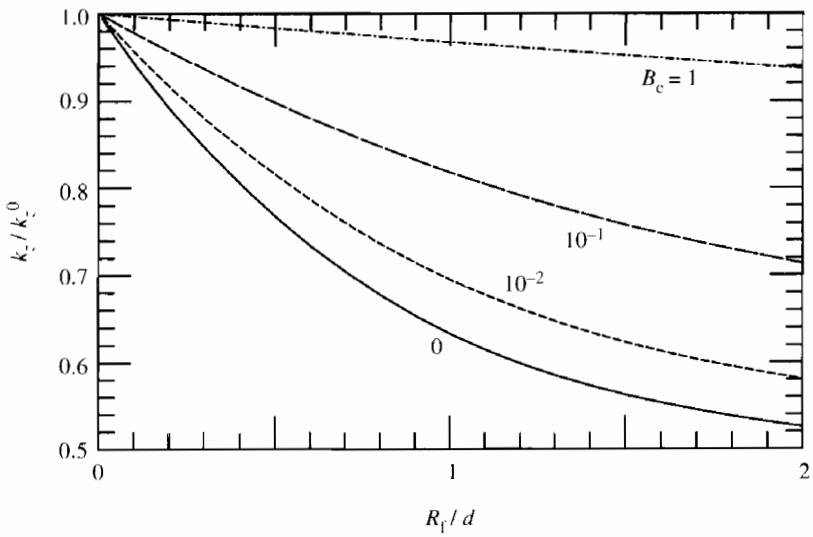

Figure 4. The effect of varying the Biot number for matrix cracking on the overall longitudinal thermal conductivity for $k_z^f/k_m = 2$, $\gamma = 1$ and $\rho = 0.3$.

but clearly its value should be assigned consistent with the ambient temperature in the composite.

The temperature gradient averaged across the fibre is still given by (3.3). From (2.8) and (3.3), the temperature gradient in the matrix immediately follows as

$$\hat{T}_{m,z} = -\frac{q_z^0}{k_z^0} - \frac{\rho k_z^f A_1}{(1-\rho)k_m} \cosh\left(\xi \frac{z}{R_f}\right) \quad \text{for} \quad |z| \leqslant \tfrac{1}{2}d. \tag{3.8}$$

Given that the temperature is *uniform* with respect to r at $z = 0$ and $z = d$, it follows that the temperature drop across the crack can be expressed as

$$\begin{aligned} \hat{T}_m^+ - \hat{T}_m^- = \Delta T - 2\int_0^{d/2} \frac{\mathrm{d}\hat{T}_m}{\mathrm{d}z}\,\mathrm{d}z = 2\int_0^{d/2} \left[\frac{\mathrm{d}\hat{T}_f}{\mathrm{d}z} - \frac{\mathrm{d}\hat{T}_m}{\mathrm{d}z}\right] \mathrm{d}z \\ = \frac{2A_1 R_f k_z^0}{(1-\rho)\xi k_m} \sinh\left(\xi \frac{d}{2R_f}\right). \end{aligned} \tag{3.9}$$

When (2.17) is rewritten in terms of $\hat{T}_m$, and (3.8) and (3.9) are substituted into the result, one finds

$$A_1 = -\frac{q_z^0}{k_z^0} \frac{(1-\rho)k_m}{\rho k_z^f} \left\{\cosh\left(\xi \frac{d}{2R_f}\right) + \frac{2k_z^0 H_g R_f}{\rho \xi k_m k_z^f} \sinh\left(\xi \frac{d}{2R_f}\right)\right\}^{-1}. \tag{3.10}$$

Finally, the overall longitudinal thermal conductivity of the composite is obtained from relations (2.10), (3.3) and (3.10) as

$$k_z = k_z^0 \left\{1 + \frac{(1-\rho)k_m}{\rho k_z^f} \frac{\tanh(\xi d/2R_f)/(\xi d/2R_f)}{1 + (2k_z^0 B_c/\rho\xi k_m)\tanh(\xi d/2R_f)}\right\}^{-1}, \tag{3.11}$$

where $B_c = H_c R_f / k_z^f$ is the Biot number for matrix cracking. Relation (3.11) reduces to (3.8) for adiabatic crack surfaces ($H_c = 0$).

The effect of B_c on the normalized overall thermal conductivity, k_z/k_z^0, is il-

Table 1. *The properties of dry air at atmosphere pressure*
(The dimension of H_g is W m^{-2} K^{-1}.)

T (K)	l_m (10^{-8} m)	k_g (W m^{-1} K^{-1})	$\delta = 0.01$ μm	$\delta = 0.1$ μm	$\delta = 1$ μm
300	5.69	0.032	$N_K = 5.69$ $H_g = 3.2 \times 10^6$	$N_K = 0.57$ $H_g = 3.2 \times 10^5$	$N_K = 0.057$ $H_g = 3.2 \times 10^4$
1273	11.1	0.085	$N_K = 11.1$ $H_g = 8.5 \times 10^6$	$N_K = 1.11$ $H_g = 8.5 \times 10^5$	$N_K = 0.11$ $H_g = 8.5 \times 10^4$

lustrated in figure 4, for $k_z^f/k_m = 2$, $\gamma = 1$ and $\rho = 0.3$. The limit for $B_c = 0$ corresponds to perfectly insulating cracks for which results have been displayed previously, while the limit for $B_c = \infty$ leaves the overall conductivity unchanged at k_z^0. The value of B_c characterizing the transition midway between these two extremes is about 0.1. To acquire some feel for the significance of crack thermal conductance, consider a ceramic composite with a fibre of radius, $R_f = 10$ μm, and conductivity in the range 10^2 10^3 W m^{-1} K^{-1} expected for SiC fibres. If B_c is to be greater than 0.1, the crack conductance parameter, H_c, must be larger than 10^6–10^7 W m ^{2} K ^{1}. As already discussed, the contribution of H_r to H_c is likely to be orders of magnitude smaller than this. To gain some insight into the contribution from H_g, consider the parameter values for dry air at a pressure of one atmosphere given in table 1 for $T = 300$ K and $T = 1273$ K, taken from Scars (1967). The mean free path of the molecules in the gas, l_m, is on the order of 0.1 μm at both temperatures giving rise to the Knudsen number, N_K, shown for each of the three values of the crack opening, δ. The continuum conductance of the gas k_g is not applicable to the two smallest crack openings at $\delta = 0.01$ μm and 0.1 μm. Nevertheless, even for these cases, the continuum formula $H_g = k_g/\delta$ should give a rough estimate of the heat conductance across the crack, an estimate which is expected to be somewhat below the value appropriate in the regime of intermediate to large Knudsen numbers. It can be seen from the values of H_g given in table 1 that B_c is likely to be as large as 0.1 when the crack openings are in the range from 0.01 μm to somewhat less than 0.1 μm, but B_c should be well below 0.1 for 'large' openings of 1 μm. From this example, we conclude that composite thermal conductivity may be sensitive to conductance by the gas in the matrix cracks, with cracks with openings well above 0.1 μm acting as barriers to thermal conduction and those with openings below 0.1 μm having less effect on the overall heat flow.

4. Thermal conductivity of cracked composites with partly or fully debonded interfaces

In this section the combined effects of matrix cracking and thermal contact resistance due to fibre–matrix debonding on the overall longitudinal thermal conductivity of the composite are considered. The thermal barrier at the debonded interface may be modelled either by an equivalent interfacial heat transfer coefficient h_i or by introducing a thin cylindrical layer of poor conductivity between the fibre and the matrix. The concept of interfacial heat transfer in the form of

(2.11) will be adopted below due to its simplicity. As discussed, the coefficient h_i depends on surface asperities, thermal expansion mismatch, gas in the interface, interface temperature and possibly other factors. As in the study of the effect of matrix crack conductance, h_i will be taken to be independent of temperature in the analysis.

For the bonded portion of the fibre, the differential equation (3.1) governing the longitudinal temperature gradient has a solution in the form,

$$\hat{T}_{f,z} = -q_z^0/k_z^0 + A_2 \cosh(\xi z/R_f) \quad \text{for} \quad |z| \leqslant \tfrac{1}{2}d - l, \tag{4.1}$$

where the unknown coefficient A_2 will be determined from the continuity of $\hat{T}_{f,z}$ at the debond tip. For the debonded portion of the fibre, the analysis gives

$$\frac{d^2\hat{T}_{f,z}}{dz^2} = \left(\frac{\zeta}{R_f}\right)^2 \left(\hat{T}_{f,z} + \frac{q_z^0}{k_z^0}\right) \quad \text{for} \quad \tfrac{1}{2}d - l \leqslant |z| \leqslant \tfrac{1}{2}d, \tag{4.2}$$

where the dimensionless coefficient ζ is related to ξ by

$$\zeta = \xi \left\{\frac{1}{1 + 4\gamma/B_i}\right\}^{1/2}, \tag{4.3}$$

and $B_i \equiv h_i R_f/k_z^f$ is the Biot number for the debonded interface. The limiting case of $B_i \to 0$ represents the *adiabatic* boundary condition in which the debonded portion of the fibre–matrix interface is perfectly insulated. The other limit $B_i \to \infty$ refers to the case where *intimate thermal contact* obtains between the fibre and matrix with $T_{fi} = T_{mi}$ everywhere across the debonded interface; then, (4.2) reduces to (3.1). The general solution to (4.2) for a gradient which is symmetric with respect to $z = 0$ is

$$\hat{T}_{f,z} = -q_z^0/k_z^0 + A_3 \cosh(\zeta z/R_f) \quad \text{for} \quad \tfrac{1}{2}d - l \leqslant |z| \leqslant \tfrac{1}{2}d, \tag{4.4}$$

where the unknown coefficient A_3 will be determined from the boundary condition on the matrix crack surface.

(a) *Thermally insulating matrix cracks*

If debonding of length l has occurred at the fibre–matrix interface and no heat is being transferred across the matrix cracks, combination of relations (4.1), (4.4) with relations (2.8), (2.11) and (2.18) gives the following distribution of average temperature gradient within the fibre

$$\hat{T}_{f,z} = \begin{cases} -\dfrac{q_z^0}{k_z^0}\left\{1 + \dfrac{1-\rho}{\rho}\dfrac{k_m}{k_z^f}\dfrac{\cosh[\zeta(\frac{1}{2}d - l)/R_f]}{\cosh[\xi(\frac{1}{2}d - l)/R_f]}\dfrac{\cosh(\xi z/R_f)}{\cosh(\zeta d/2R_f)}\right\}, \\ \qquad \text{for} \quad |z| \leqslant \tfrac{1}{2}d - l, \\ -\dfrac{q_z^0}{k_z^0}\left\{1 + \dfrac{1-\rho}{\rho}\dfrac{k_m}{k_z^f}\dfrac{\cosh(\zeta z/R_f)}{\cosh(\xi d/2R_f)}\right\}, \\ \qquad \text{for} \quad \tfrac{1}{2}d - l \leqslant |z| \leqslant \tfrac{1}{2}d. \end{cases} \tag{4.5}$$

The resulting expression for the effective overall longitudinal thermal conductivity of the composite becomes

$$k_z = k_z^0 \left\{1 + \frac{1-\rho}{\rho}\frac{k_m}{k_z^f}\left[\frac{\tanh(\zeta d/2R_f)}{\zeta d/2R_f} + F\left(\xi, \zeta, \frac{l}{R_f}, \frac{d}{R_f}\right)\right]\right\}^{-1}. \tag{4.6}$$

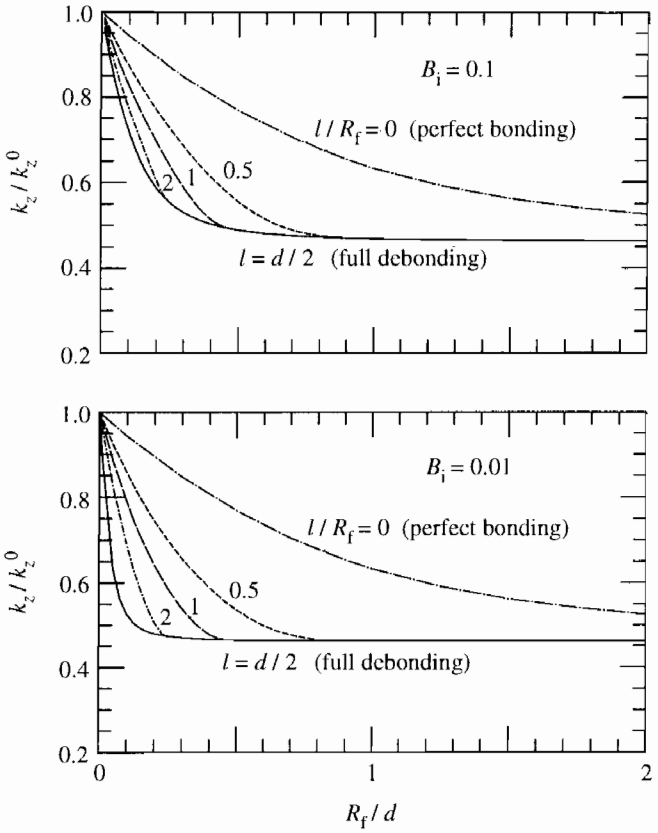

Figure 5. Effect of fibre matrix debonding on the overall longitudinal thermal conductivity of the cracked unidirectional composite for (*a*) $B_i = 0.1$ and (*b*) $B_i = 0.01$. The constitutive parameters used are $k_z^f/k_m = 2$, $\gamma = 1$, $\rho = 0.3$ and $B_c = 0$.

Here, F is a dimensionless function defined by

$$F\left(\xi, \zeta, \frac{l}{R_f}, \frac{d}{R_f}\right) = \frac{\cosh[\zeta(\frac{1}{2}d - l)/R_f]}{\cosh(\zeta d/2R_f)} \left\{ \frac{\tanh[\xi(\frac{1}{2}d - l)/R_f)}{\xi d/2R_f} - \frac{\tanh[\zeta(\frac{1}{2}d - l)/R_f)}{\zeta d/2R_f} \right\}. \quad (4.7)$$

The predicted values of k_z/k_z^0 are plotted in figure 5 against R_f/d for five choices of normalized debond length: $l/R_f = 0$, 0.5, 1, 2, $d/2R_f$, and two values of the interface Biot number: $B_i = 0.01$ and 0.1. The parameters $k_z^f/k_m = 2$, $\rho = 0.3$ and $\gamma = 1$ have been used in plotting these curves. Compared with the case of matrix cracking unaccompanied by fibre–matrix debonding where a fairly high density of cracks is needed to cause a significant reduction in the axial thermal conductivity k_z, the results in figure 5 clearly show that debonding associated with a low Biot number can reduce k_z to the lowest limit, ρk_z^f, even at relatively low crack densities.

At full debonding, when $l = \frac{1}{2}d$, F vanishes in (4.6), yielding

$$k_z = k_z^0 \left\{ 1 + \frac{1 - \rho}{\rho} \frac{k_m}{k_z^f} \left[\frac{\tanh(\zeta d/2R_f)}{\zeta d/2R_f} \right] \right\}^{-1}, \quad (4.8)$$

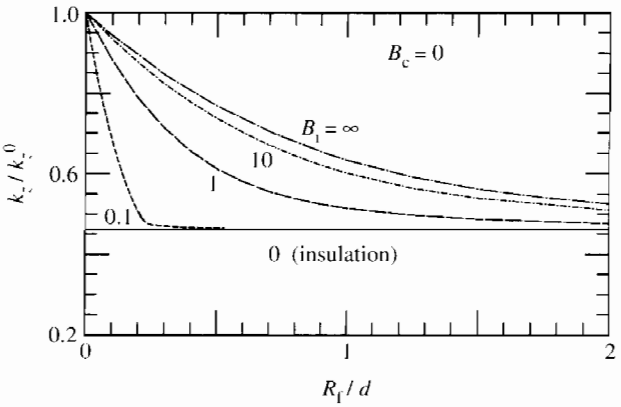

Figure 6. The effect of varying the interfacial Biot number B_i on the overall longitudinal thermal conductivity of the cracked unidirectional composite with complete debonding over the fibre–matrix interface. The constitutive parameters used are the same as those listed in figure 5.

which has the same form as that of (3.8) for the case of perfect bonding except that the coefficient ξ there is now replaced by ζ. Moreover, (4.8) reduces to (3.6) when the fibre and matrix are in intimate contact across the debonded portion of the interface ($B_i = \infty$). If the debonded interfaces are perfectly insulating ($B_i = 0$), k_z reduces to ρk_z^f for all crack spacing d. For intermediate values of B_i, the curve of k_z/k_z^0 against R_f/d is plotted in figure 6, again with $k_z^f/k_m = 2$, $\rho = 0.3$ and $\gamma = 1$. For composite systems having values of $B_i < 0.1$, the conclusion to be drawn from figure 6 is that the debonded portion of the interface can be safely taken to be perfectly insulating.

(*b*) *The combined effect of* B_i *and* B_c

If heat is transmitted across the matrix crack surfaces ($B_c > 0$), the solution for A_2 and A_3 follows along the lines outlined in § 3 and for the case just discussed. The result is

$$A_2 = A_3 \frac{\cosh[\zeta(\frac{1}{2}d - l)/R_f]}{\cosh[\xi(\frac{1}{2}d - l)/R_f)}, \tag{4.9}$$

$$A_3 = -\frac{q_z^0}{k_z^0} \frac{(1-\rho)k_m}{\rho k_z^f \cosh(\zeta d/2R_f)} \left\{1 + \frac{2k_z^0 H R_f}{\zeta \rho k_m k_z^f} \tanh\left(\frac{\zeta d}{2R_f}\right)\right\}^{-1}. \tag{4.10}$$

The corresponding solution for the overall conductivity k_z is

$$k_z = k_z^0 \left\{1 + \frac{(1-\rho)k_m}{\rho k_z^f} \frac{\tanh(\zeta d/2R_f)/(\zeta d/2R_f) + F(\xi, \zeta, l/R_f, d/R_f)}{1 + (2k_z^0 B_c/\zeta \rho k_m)\tanh(\zeta d/2R_f)}\right\}^{-1}, \tag{4.11}$$

where ζ depends on B_i as given by (4.3) and F is still given by (4.7). In the case of complete debonding along the interface ($l = \frac{1}{2}d$), $F = 0$ and (4.11) becomes formally identical to (3.11) except for the replacement there of ξ by ζ.

With B_i fixed at 0.1 and with $k_z^f/k_m = 2$, $\rho = 0.3$ and $\gamma = 1$, the values of k_z/k_z^0 from (4.11) are displayed in figure 7 for several choices of B_c, assuming that full debonding has taken place along the fibre–matrix interface. They are bracketed by the two limiting cases $B_c = 0$ and $B_c = \infty$ corresponding to $k_z = \rho k_z^f$ and $k_z = k_z^0$, respectively. Apparently, if the magnitudes of both B_i and B_c are

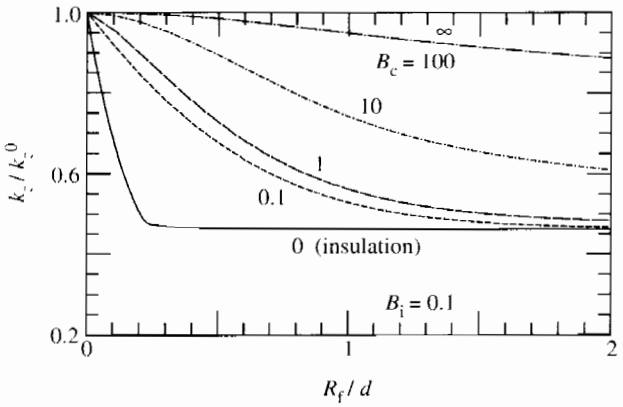

Figure 7. The effect of varying the matrix cracking Biot number B_c on the overall longitudinal thermal conductivity of the cracked unidirectional composite with complete debonding over the fibre–matrix interface. The constitutive parameters used are $k_z^f/k_m = 2$, $\gamma = 1$, $\rho = 0.3$ and $B_i = 0.1$.

less than 0.1, then the approximations of *adiabatic* crack surfaces and *adiabatic* debonded interfaces can be justified.

5. Concluding remarks

Matrix cracking in combination with interfacial debonding can reduce the overall longitudinal thermal conductivity of a unidirectional fibre-reinforced composite to a level where essentially all the heat is conducted through the fibres. The reduction can be as large as 50–70% if the fibre conductivity is comparable to that of the matrix and the volume fraction of the fibre is in the range of 0.3–0.5. Significantly, this can be achieved at relatively low crack densities when extensive debonding occurs, if the relevant Biot numbers for the matrix cracks and the debonded interfaces are both less than about 0.1. In the case where matrix cracking is not accompanied by fibre debonding, correspondingly large reductions in the thermal conductivity of the composite are not seen until the cracks reach a relatively high density rarely observed in practice. Matrix cracking perpendicular to the fibres does not affect the transverse heat-carrying capability of the composite if the fibres are perfectly bonded to the matrix.

Insightful discussions by one of the us (T.J.L.) with Professor H. W. Emmons and Professor J. L. Sanders, Jr, concerning heat transfer boundary conditions have been very helpful. Financial support from ARPA University Research Initiative (Subagreement P.O. #KK 3007) with the University of California, Santa Barbara, ONR Prime Contract N00014-92-J-1808, and from the Division of Applied Sciences, Harvard University, is gratefully acknowledged. The finite-element code, ABAQUS, was used to provide selected numerical solutions to the cell model.

References

Batchelor, G. K. 1974 *A. Rev. Fluid Mech.* **6**, 227–251.

Beyerle, D., Spearing, S. M., Zok, F. W. & Evans, A. G. 1992 *J. Am. Ceram. Soc.* **75**, 2719–2725.

Bhatt, H., Donaldson, K. Y., Hasselman, D. P. H. & Bhatt, R. T. 1990 *J. Am. Ceram. Soc.* **73**, 312–316.

Benveniste, Y. 1987 *J. appl. Phys.* **61**, 2840–2843.

Fadale, T. D. & Taya, M. 1991 *J. Mater. Sci. Lett.* **10**, 682–684.

Hasselman, D. P. H. 1978 *J. Comp. Mater.* **12**, 403–407.

Hasselman, D. P. H. & Johnson, L. F. 1987 *J. Comp. Mater.* **21**, 508–512.

He, M. Y., Wu, B.-X., Evans, A. G. & Hutchinson, J. W. 1994 *Mech. Mater.* **18**, 213–229.

Hoenig, A. 1983 *J. Comp. Mater.* **17**, 231–237.

Hutchinson, J. W. & Jensen, H. M. 1990 *Mech. Mater.* **9**, 139–163.

Laws, N. & Dvorak, G. J. 1988 *J. Comp. Mater.* **22**, 900–916.

Leung, W. P. & Tam, A. C. 1988 *J. appl. Phys.* **63**, 4505–4510.

Lu, T. J. & Hutchinson, J. W. 1995 *Composites.* (In the press.)

McCartney, L. N. 1992 *J. Mech. Phys. Solids* **40**, 27–68.

Sears, F. W. 1967 *Introduction to thermodynamics: the kinetic theory of gases and statistical mechanics.* Cambridge, MA: Addison-Wesley.

Swartz, E. T. & Pohl, R. O. 1989 *Rev. mod. Phys.* **61**, 605–668.

Tzou, D. Y. 1991 *J. Comp. Mater.* **25**, 1064–1084.

Tzou, D. Y. & Li, J. 1993 *Int. J. Heat Mass Transfer* **36**, 3887–3895.

Discussion

D. J. RÖDEL (*GDP, Darmstadt, Germany*). Could Professor Hutchinson get an insight into asperity contact and especially into the change of asperity contact after cyclic loading from thermal conductivity measurements in transverse directions on uniaxial debonded reinforcements?

J. W. HUTCHINSON. This seems quite possible. There is only one set of data, from Hasselman. They measured transverse conductivity in vacuum and argon and from the data in argon one could get an insight into asperity contact. The micromechanics would not help much—you would have to calibrate.